Pergamon

0961–9534(94)00040–9

Biomass and *Bioenergy* Vol. 7, Nos. 1-6, pp. 87-98. 1994

0961-9534/94 $7.00 + 0.00

NUMERICAL SIMULATION OF CELLULOSE PYROLYSIS

COLOMBA DI BLASI

Dipartimento di Ingegneria Chimica, Università degh Studi di Napoli Federico II, Piazzale V. Tecchio, 80125 Napoli, Italy

Abstract-A mathematical model of transport phenomena and chemical processes of the thermal degradation of cellulose is presented. The kinetic model developed by Bradbury et al. (J. *Appl. Polym. Sci.* **23,** 3271, 1979) for primary pyrolysis is extended to include secondary reactions of volatiles:

$$\text{Cellulose} \xrightarrow{k_1} \text{Active cellulose} \begin{cases} \xrightarrow{k_3} \text{Tar} \xrightarrow{k_4} \text{Gas} \\ \xrightarrow{k_2} \text{Char} + \text{Gas}. \end{cases}$$

From the physical point of view, the model describes convective, conductive and radiative heat transfer, mass convection and diffusion and velocity and pressure variations interior to the porous solid (Darcy law). Furthermore, porosity, mass diffusivity, permeability and thermal conductivity vary with the composition of the reacting medium. Time and space evolution of the main variables, and reaction product distribution, are simulated by varying the reactor temperature and the reactor heating rate.

Keywords-Modeling; cellulose; pyrolysis; heat transfer.

INTRODUCTION

Cellulose is the main component of wood and biomass fuels. Consequently, a better understanding of the role played by physical and chemical processes during its thermal degradation represents the first step towards the development of pyrolysis models of complex solid fuels. The approach to the pyrolytic behavior of biomass fuels as a weighted average of the pyrolytic behavior of the main components (cellulose, hemicellulose and lignin) has been widely used in the literature.[1–5] Chemical processes of biomass pyrolysis can be identified as two main stages, that is, primary degradation of the virgin material to a solid charred residual (char), low molecular weight gaseous species (gas) and condensable organic components (tar), and secondary degradation of evolved products.

Thermal degradation of cellulose may occur under a chemically controlled regime or under a heat transfer controlled regime.[6] In the first case, the heat transfer rate is much larger than the overall reaction rate, and chemical processes, which occur under nearly isothermal conditions, control particle conversion. Under heat transfer regime conditions, strong temperature gradients are established along the particle and the conversion process results from a strong coupling between transport phenomena and chemical reactions. Generally, the heat transfer regime is associated with the conversion of large particles which are preferred for feeding biomass reactors because of the high cost of size reduction.

Models of the heat transfer controlled regime of cellulosic material pyrolysis published to date use simplifying assumptions for the description of both chemical processes and transport phenomena. In most cases, chemical processes have been described by a one-step, first-order, Arrhenius reaction.[7–10] The predictive capabilities of such models are strongly limited by the need to assign the final char density and thus the total char yield. Computer models of biomass pyrolysis under heat transfer controlled regime conditions, which describe chemical processes through multi-step reaction schemes, with the assumption of lumping the products of decomposition into tar, char and gas, are also available. Recently, two models of cellulose pyrolysis including only primary" and both primary and secondary reactions[12] have been proposed. Primary and secondary reactions of large wood particles' pyrolysis have also been modeled.[13,14]

A different degree of approximation has been employed in the modeling of transport phenomena. In general the analyses take the viewpoint

that the porosity is fine and uniformly distributed. The material is considered as a homogeneous medium where gas and solid are in good thermal contact (solid and gas are at the same temperature). Some of the models accounting for multi-step pyrolysis reaction schemes do not consider pressure variations,[11-13] convective transport of tar species generated during the reaction process[11,13] or make the assumption of quasi-steady gas phase processes.[11-13] The most recent contribution in the modeling of multi-step wood pyrolysis accounts for all main physical processes.[14] Unsteady gas-phase processes, heat transfer through convection, conduction and radiation, volatile species (including tar) convection, effects of pressure gradients and variable properties have been described. The analysis of the problem of wood pyrolysis[14] is, however, in some way limited by the use of a rough estimation of kinetic data derived from Ref. [15].

The present contribution couples the description of all these physical processes,[14] improved through the description of chemical species diffusive transport, to a well-established multi-step reaction scheme of cellulose pyrolysis,[16] extended to include secondary reactions." Thus, the model represents the first step towards the development of more accurate models of large biomass particle pyrolysis based on the contributions of the single biomass components. The model is also used to predict the dependence of the product yields from cellulose pyrolysis on the reactor temperature and reactor heating rate. Indeed, two different objectives" have been pursued in the analysis of the fast pyrolysis of biomass fuels, that is, the production of the maximum yield of gases (ethylene or other olefins) or the production of the maximum yield of liquids. The attainment of either goal is strongly dependent on the reaction conditions. In general, processes characterized by high temperatures (>920 K) and long residence times are aimed at obtaining high yields of gases, whereas processes for the attainment of high liquid yields operate at much lower temperatures (720-820 K), and with reduced vapor residence times.

THE MODEL OF CELLULOSE PYROLYSIS

According to the analyses by Broido and coworkers[19] thermal degradation of cellulose starts at about 490 K with endothermic intermolecular water elimination to produce anhydrocellulose, whereas endothermic tar (essentially levoglucosan) formation predominates at higher temperature (about 550 K). The anhydrocellulose undergoes further exothermic pyrolysis to form char and gases. A subsequent study by Arseneau,[20] based on the analysis of the thermograms of cellulose and levoglucosan, confirmed only partially the findings of Broido and coworkers.[19] For the case of thin cellulose samples, only endothermic processes were observed, whereas for thick cellulose samples and levoglucosan a strong exotherm was observed for the range of temperature 570-620 K. This behaviour led to the conclusion that the anhydrocellulose is highly reactive and rapidly undergoes further reactions with gas and char formation. However, such processes are not exothermic, while the levoglucosan decomposes exothermically. Thus, the exotherm observed at high temperatures during the pyrolysis of thick cellulose samples is the result of secondary reactions and not representative of primary pyrolysis processes.

The degradation of cellulose was also extensively investigated by Shafizadeh and coworkers[16] in the temperature range 530-610 K. Similar to the Broido analyses, two main pathways were found. The first pathway, which dominates at low temperatures, involves reduction in the degree of polymerization by bond scission, appearance of free radicals, elimination of water, formation of low molecular weight gases and a char residue. At temperatures of about 570 K, the second pathway starts to become competitive and rapidly dominates. The primary reaction in this pathway involves depolymerization by transglycosylation, followed by dehydration and formation of char and gas. As the temperature is increased, the tar forming reactions accelerate rapidly and overshadow the formation of char and gases. The chemical kinetics of the process, represented by the following scheme:

$$\text{Cellulose} \xrightarrow{k_1} \text{Active cellulose} \qquad \text{(a1)}$$

$$\text{Active cellulose} \xrightarrow{k_2} \text{Char} + \text{Gases} \qquad \text{(a2)}$$

$$\text{Active cellulose} \xrightarrow{k_3} \text{Tar} \qquad \text{(a3)}$$

are used in this study.

In general, secondary reactions describe tar degradation to light gases and/or condensation to solid or refractory condensable ma-

terials.[17,21,22] In agreement with some experimental observations,".** the present analysis assumes that first-order tar degradation occurs to light gases:

$$\text{Tar} \xrightarrow{k_4} \text{Gas}. \qquad \text{(a4)}$$

The kinetic equations for chemical species, participating in reactions (a1)–(a4), are as follows:

$$\frac{\partial \rho_W}{\partial t} = -K_1 \rho_W, \qquad (1)$$

$$\frac{\partial \rho_A}{\partial t} = K_1 \rho_W - (K_2 + K_3)\rho_A, \qquad (2)$$

$$\frac{\partial \rho_C}{\partial t} = \nu_C K_2 \rho_A, \qquad (3)$$

$$\frac{\partial \rho_T \epsilon}{\partial t} = K_3 \rho_A - \epsilon K_4 \rho_T, \qquad (4)$$

$$\frac{\partial \rho_G \epsilon}{\partial t} = \nu_G K_2 \rho_A + \epsilon K_4 \rho_T, \qquad (5)$$

where $K_k = A_k \exp(-E_k/RT)$ $(k = 1, 4)$, $\rho_W = M_W/V, \rho_A = M_A/V, \rho_C = M_C/V$, are the apparent cellulose, active cellulose and char densities, $\rho_T = M_T/V_g = M_T/(\epsilon V), \rho_G = M_G/V_g = M_G/(\epsilon V)$, the mass concentrations of volatile species (tar and gas, respectively) and $\epsilon = V_g/V$ the porosity of the medium.

The formation of active cellulose is modeled as an isothermal process.'* Unlike Refs [12,19] and according to Ref. [20], tar formation (a3) is described as an endothermic process. Reaction (a2) (linked char and gas formations) is assumed to occur endothermically" and finally tar degradation (a4) is a mildly exothermic process.[20]

Kinetic data and values of the heat of pyrolysis, used in the simulations, are summarized in Table 1.

Table 1. Kinetic data and property values

Kinetic data	
$A_1 = 2.8 \times 10^{19}\,s^{-1}$	Bradbury et *al.* (1979)
$A_2 = 1.3 \times 10^{10}\,s^{-1}$	Bradbury *et al.* (I 979)
$A_3 = 3.28 \times 10^{14}\,s^{-1}$	Bradbury *et a/.* (1979)
$A_4 = 4.28 \times 10^{6}\,s^{-1}$	Liden *et al.* (1988)
$E_1 = 242.4$ kJ/mol	Bradbury *et al.* (I 979)
$E_2 = 150.5$ kJ/mol	Bradbury *et al.* (1979)
$E_3 = 196.5$ kJ/mol	Bradbury *et al.* (1979)
$E_4 = 108$ kJ/mol	Liden et *al.* (1988)
$\Delta h_1 = 0$	Curtiss and Miller (1988)
Ah, = Ah, = 418 kJ/kg	Di Blasi (1993)
Ah, = -42 kJ/kg	Curtiss and Miller (1988)
$\nu_G = 0.65$	Bradbury *et al.* (1979)
$\nu_C = 0.35$	Bradbury et *al.* (1979)
Property values	
$\rho_{W0} = 420$ kg/m^3	Curtiss and Miller (1988)
$c_W = c_A = 2.3$ kJ/kgK	Curtiss and Miller (1988)
$c_T = 2.5$ kJ/kgK	Curtiss and Miller (1988)
$c_g = 1.1$ kJ/kgK	Di Blasi (1993)
cc = 1.1 kJ/kgK	Curtiss and Miller (1988)
$d = 4 \times 10^{-5}$ m	Chan et *al.* (1985)
$k_W = 24.26 \times 10^{-2}$ W/mK	Curtiss and Miller (1988)
kc = 10.46 x 10^{-2} W/mK	Di Blasi (1993)
$k_g = 25.77 \times 10^{-3}$ W/mK	Di Blasi (1993)
$\mu = 3 \times 10^{-5}$ kg/ms	Kansa *et al.* (1977)
$\omega = 1$	Chan *et al.* (1985)
$h_{conv} = 20$ W/m^{2}K	Lee et *al.* (1976)

MODEL EQUATIONS

The physical problem under study is that of a one-dimensional cellulose particle in an inert atmosphere subjected on both sides to known temperature and pressure fields (reactor conditions). The reacting medium is modeled as a solid matrix where the void volume, formed by pores, is initially filled by an inert gas. As a result of the pyrolysis *process,* gaseous species and a solid residual are formed while medium properties (porosity, permeability, mass diffusivity, thermal conductivity and heat capacity) change. Some assumptions are made in the formulation of the mathematical model. The possible tar and water condensation, after migration from the high-temperature pyrolysis region to the low-temperature region of the virgin cellulose, is not accounted for. Thermal swelling and/or shrinkage and surface regression are neglected, that is $V = V_s(t) + V_g(t) = \text{const}$. Gaseous products of solid degradation are assumed to reach the gas phase instantaneously. The flow velocity, established through the porous structure of the solid, is the result of volatile release rate and pressure gradients. Finally the gas and the solid matrix are in local thermal equilibrium.

Mass balances for solid-phase species, cellulose, active cellulose and char, are given by eqns (1)–(3). As for gas-phase species, by neglecting the contribution of the inert initially present in the pores of the solid matrix, a conservation equation for tar and the total continuity equation are considered:

-mass balance for tar species

$$\frac{\partial(\epsilon\rho_T)}{\partial t} + \frac{\partial(\rho_T u)}{\partial x} = \omega_T + \frac{\partial}{\partial x}\left(\rho_g D \frac{\partial Y_T}{\partial x}\right), \qquad (6)$$

where $\omega_T = K_3 \rho_A - \epsilon K_4 \rho_T$.

-total continuity

$$\frac{\partial(\epsilon\rho_g)}{\partial t} + \frac{\partial(\rho_g u)}{\partial x} = \omega_g, \qquad (7)$$

where $\rho_g = \rho_G + \rho_T$ and $\omega_g = (v_G K_2 + K_3)\rho_A$ and g is the subscript to indicate total volatiles (gas + tar).

The energy balance can be written with the assumptions of negligible kinetic and potential energy and by the replacement of the internal energy with enthalpy:[14]

$$\frac{\partial}{\partial t}[\rho_C h_C + \rho_W h_W + \rho_A h_A + \epsilon(\rho_G h_G + \rho_T h_T)] + \frac{\partial}{\partial x}[(\rho_T h_T + \rho_G h_G)u] = \frac{\partial}{\partial x}\left(k^* \frac{\partial T}{\partial x}\right) - \sum_{k=1,3} r_k \Delta h_k - \epsilon r_4 \mathrm{Ah}, \quad (8)$$

where

$$r_1 = A_1 \exp(-E_k/RT)\rho_W,$$
$$r_k = A_k \exp(-E_k/RT)\rho_A \quad (k = 2,3),$$
$$r_4 = A_4 \exp(-E_k/RT)\rho_T,$$
$$h_W = c_W(T - T_0), \; h_A = c_A(T - T_0),$$
$$h_T = c_T(T - T_0), \quad h_C = c_C(T - T_0),$$
$$h_G = c_G(T - T_0).$$

Furthermore, the effective thermal conductivity consists of a conductive and a radiative contribution: $k^* = k_{con} + k_{rad}$, where $k_{rad} = \sigma T^3 d/\omega$.[13] This expression is obtained through a radiative heat transfer balance, considering the pores as spheres (diameter, d), one-half of which is at uniform temperature T and the other half at T' and for small values of the ratio $(T - T')/T$.

Momentum transfer is described according to the Darcy law:

$$u = -\frac{K}{\mu}\frac{\partial p}{\partial x}. \quad (9)$$

The mixture of gases inside the porous solid behaves according to the ideal gas law:

$$p = \frac{\rho_g R T}{W_g}. \quad (10)$$

Finally, the equation describing the time evolution for V_s is written assuming that:

$$\frac{V_s}{V_{s0}} = \frac{(M_W + M_A + M_C)}{M_{W0}}. \quad (11)$$

Properties of the virgin cellulose and active cellulose are assumed to be the same. However, as thermal degradation occurs, they, as well as the pore diameter, vary linearly with the medium composition from the initial values (cellulose and active cellulose) to the final values of char residual:[7,8,14]

$$k_{con} = \eta k_W + (1 - \eta)k_C + \epsilon k_g, \quad (12)$$
$$D = \eta D_W + (1 - \eta)D_C, \quad (13)$$
$$K = \eta K_W + (1 - \eta)K_C, \quad (14)$$
$$d = \eta d_W + (1 - \eta)d_C, \quad (15)$$

where $\eta = (M_W + M_A)/M_{W0}$.

In order to define the problem, initial and boundary conditions should also be assigned. The cellulose sample is located in a reactor whose temperature T_{rea} is made to increase, with an assigned rate to a final value T_r, whereas the pressure is assumed constant and equal to the ambient value (p_0).

Initially $(t = 0)$ the cellulose sample is at ambient conditions:

$$T = T_0, \quad \rho_W = \rho_{W0}, \quad p = p_0, \quad u = 0. \quad (16)$$

At the surface of the particle (x = L), radiant and convective heat transfer and constant ambient pressure conditions are used:

$$k^* \frac{\partial T}{\partial x} = -\sigma e (T^4 - T_{rea}^4) - h_{conv}(T - T_{rea}); \; p = p_0, \quad (17)$$

whereas symmetry conditions are applied at the other side of the sample (x = 0):

$$\frac{\partial T}{\partial x} = 0, \quad \partial p/\partial x = 0 \quad (u = 0). \quad (18)$$

The convective heat transfer coefficient, h_{conv}, is assigned as determined[23] from the pyrolysis of wood at fire-level heat fluxes. The finite difference formulation of the mathematical model is based on the hybrid scheme and a two-step splitting procedure is used for the treatment of chemical processes and transport phenomena.

Results of numerical simulation of cellulose pyrolysis

In this study results of simulations of the pyrolysis of a large ($L = 2.5 \times 10^{-2}$ m) particle of cellulose are presented. The property values, used in the simulations, are listed in Table 1. The simulations are made increasing the reactor temperature from 450 K, with an assigned rate, to a fixed final value (T_r, reactor temperature), while the cellulose particle is assumed to be initially at a temperature of 300 K. The product yields and the time and space evolution of the main variables characterizing the process are predicted, as the heating rate of the reactor is

varied from 0.25 to 15 K s^{-1} and the final reactor temperature from 550 to 1500 K. The reactor temperatures have been chosen in the range of those used in the experiments of cellulose conversion through a fluidized bed reactor'* and the heating rates have been increased from the values used in the pyrolysis of large wood particles" to values high enough for the simulated ultimate product yields to attain constant values. The chemical reactions are assumed to be quenched as soon as tar vapors leave the surface of the charred cellulose.

An example of the predicted dynamics of a cellulose particle pyrolysis is presented through Figs 1-3, where the temperature, the mass concentrations of chemical species, the gas overpressure and the velocity are reported for certain times as functions of the particle length, as computed with a reactor heating rate of 15 K s^{-1} to a final reactor temperature of 1100 K. The pyrolysis process shows, in general, the same qualitative behavior as predicted for wood particles.[14] After the transients of the heating process, as the surface of the particle reaches a temperature of about 550 K, the primary pyrolysis process starts. The temperature at the surface and along a narrow layer rapidly attains large values while high spatial gradients are established. A narrow reaction front, which can be defined as the region where active cellulose is formed, is predicted to propagate, leaving behind a low-density char layer. As time increases, the width of the primary reaction front enlarges and the propagation speed of the reaction front decreases, because the reaction process occurs at successively lower temperatures.

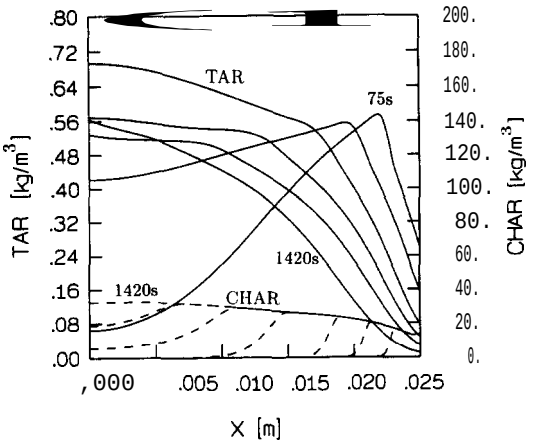

Fig. 2. Tar (solid lines) and char mass concentrations (dashed lines) as functions of the cellulose sample length for t = 75, 150, 300, 900, 1200 and 1420s (T_0 = 300 K, T_r = 1100 K, reactor heating rate 15 Ks-'). The exposed surface is at x = 0.025 m.

Indeed, the temperature, beyond a certain distance from the surface, does not exceed 650 K during the whole conversion process and such a region is not the site for secondary tar reactions. From the temperature profiles, two different regions appear: a char layer where tar degradation is an exothermic process because of both the heat of reaction and the decrease in the heat capacity from tar to gas; and a region of endothermic primary pyrolysis. For the final reactor temperatures and the pore diameter considered in the simulations, radiative heat transfer along the charred region appears to be negligible.

Besides chemical reactions and heat conduction in the pyrolysis region, the pyrolyzed gas flow introduces a convective transport which is

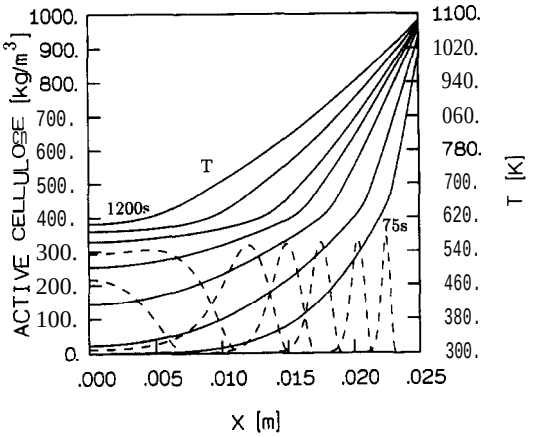

Fig. 1. Temperature (solid lines) and active cellulose mass concentration (dashed lines) as' functions of the cellulose sample length for t = 75, 150, 300, 450, 600, 900 and 1200 s (T_0 = 300 K, T_r = 1100 K, reactor heating rate 15 K s^{-1}). The exposed surface is at x = 0.025 m.

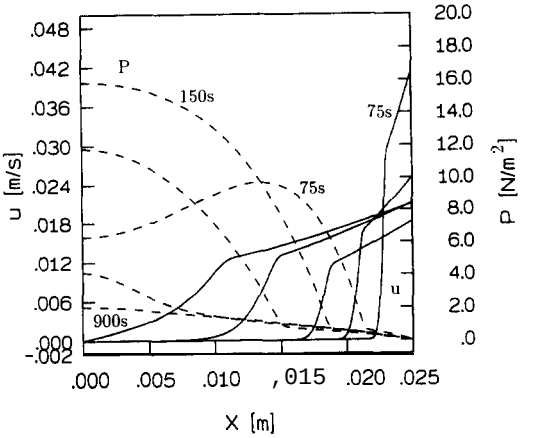

Fig. 3. Gas velocity (solid lines) and overpressure (dashed lines) as simulated along the porous structure of the cellulose sample for t = 75, 150, 300, 600 and 900 s (T_0 = 300 K, T_r = 1100 K, reactor heating rate 15 K s^{-1}). The exposed surface is at x = 0.025 m.

affected by the grain structure of the solid. Indeed, pressure gradients are established along the cellulose specimen. This indicates that the velocity characterizing the mass flow of volatiles is the result of two contributions, the first due to the net reaction production and the second to pressure variations. At very short times, the very high volatile production leads to large values of the maximum velocity (with rather large convective transport of heat out from the sample). Then, as the process becomes heat-transfer controlled, a decrease in the velocity is observed. Finally, it again increases, when the primary pyrolysis front extends to the whole sample, with larger amounts of volatiles generated. This condition corresponds to the so-called "particle heat-up time",[10,18] that is the time needed for the whole particle to reach about 95% of a temperature high enough for the initial depolymerization and the subsequent volatile species and char formation. This temperature value (reaction temperature) is about 550 K for this formulation of the cellulose pyrolysis problem. In general, pressure gradients force volatile products towards the unreacted zone as well as out of the sample. At very short times, the large permeability causes significant convective transport of volatiles across the virgin cellulose region where pressure increases. As long as a very high volatile production is observed, the overpressure in this region slightly increases with time. This is the result of a convective flow directed towards the virgin solid region and, to a lesser extent, of volatile diffusion enhanced by the strong gradients observed at the beginning of the degradation process. However, for long

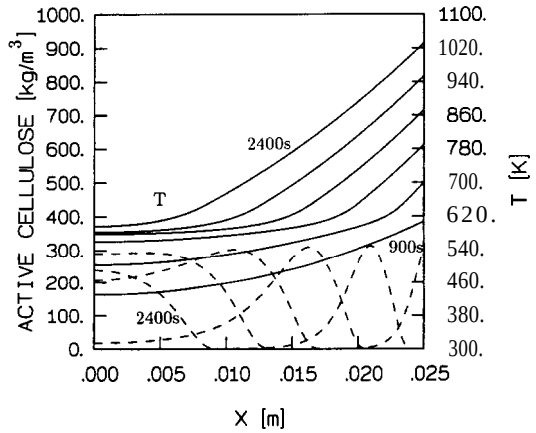

Fig. 4. Temperature (solid lines) and active cellulose mass concentration (dashed lines) as functions of the cellulose sample length from $t = 900$ s and then with step 300 s (T_0 = 300 K, T_r = 1100 K, reactor heating rate 0.25 K s^{-1}). The exposed surface is at x = 0.025 m.

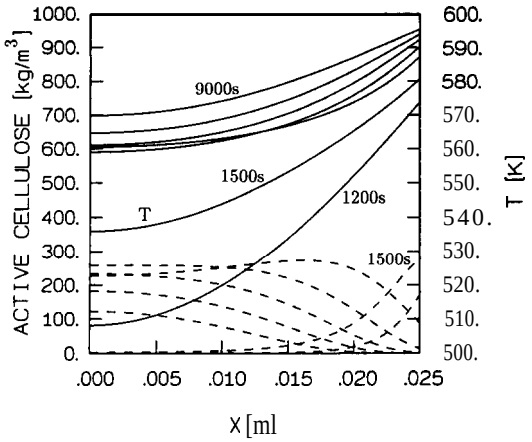

Fig. 5. Temperature (solid lines) and active cellulose mass concentration (dashed lines) as functions of the sample length from t = 1200 s, 1500 s and then with step 1500s (T_0 = 300 K, T_r = 600 K, reactor heating rate 15 K s^{-1}). The exposed surface is at x = 0.025 m.

times, the flow of volatile products occurs essentially along the already charred region, where the mass flow resistance is low.

Initially, the tar concentration attains a maximum value in the primary pyrolysis region. Then, as a consequence of strong convective and diffusive transport, it moved towards the virgin cellulose region. A strong decrease in the tar concentration is observed along the char layer because, for reactor temperatures larger than 750 K, degradation to gas occurs. At very short times, the maximum in the tar cracking rate is located at the surface of the sample, where the highest temperatures are reached and significant tar concentrations are available. Successively, the maximum decreases and the reaction zone enlarges with a slow propagation towards the interior of the particle. The variation in the local reaction temperature also affects the local char density which gradually increases with the distance from the heated surface.

The effects of reaction conditions on the detailed distribution of variables can be derived from Figs 4 and 5, where temperature and active cellulose concentrations are plotted for a lower reactor heating rate (0.25 K s^{-1}) and a lower reactor temperature (600 K). From Fig. 4, it appears that a decrease in the heating rate slows the conversion process and the width of the reaction front increases. A decrease in the spatial gradients of the main variables is also observed, but the dynamics of the process are essentially the same as previously presented for a reactor heating rate of 15 K s^{-1}. For low reactor temperatures (600 K), a further decrease in the spatial gradients of the main variables

is simulated and, apart from a thin region close to the exposed surface of the specimen, the conversion process occurs at almost the same level along the whole particle. Thus, the wave character associated with the propagation of the reaction front at high reactor temperatures is lost. The gas overpressures are noticeably reduced as well as the rate of volatile species formation with much lower gas flow velocities. A maximum of about 0.25×10^{-2} m s^{-1} is predicted, for times corresponding to the enlargement of the pyrolysis front to the whole particle thickness. After some time, a flat distribution of tar concentration is simulated, confirming again that, at these low reactor temperatures, secondary reactions do not occur at all.

From the detailed distribution of the main variables it appears that the reactor temperature plays a role of greater importance than the reactor heating rate. Indeed, for high reactor temperatures, even at very low reactor heating rates, the conversion process is always localized at a rather narrow reaction front, with rather large spatial gradients. On the contrary, for low reactor temperatures, apart from a narrow zone close to the exposed surface, the devolatilization process occurs at almost the same time for the whole cellulose thickness, with much lower gradients. In a certain way, for a large particle, whose surface is rapidly heated, both the chemical and the heat transfer regimes are observed. For a thin layer, adjacent to the surface, the heat transfer rate is large compared to the global solid degradation rate. However, the process soon becomes controlled by the rate of heat transfer to the virgin cellulose (heat transfer regime).

The reactor temperature and reactor heating rate affect the conversion process, at most, for a thickness of about 1.5×10^{-2} m. Indeed, irrespective of the reactor temperature and heating rates, the conversion process for almost 1×10^{-2} m of the particle occurs at temperatures below 650 K. In this region secondary reactions are not active.

The simulated dynamics of the solid weight loss and its rate are shown through Figs 6a and 6b for a reactor temperature of 1500 K and different reactor heating rates. For all cases, an initial period of slow weight loss is predicted, this being most noticeable for the lower heat rates. For high heating rates (> 3 K) a sharp rise in the rate of solid devolatilization, due to the fast attainment of reaction (550 K) and even higher temperature values at the surface, is

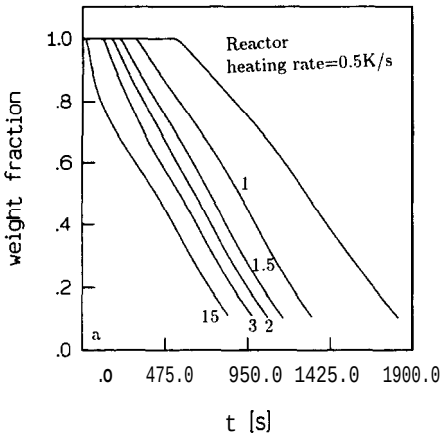

Fig. 6a. Weight fraction as function of time for several reactor heating rate [K s^{-1}] values and a final reactor temperature of 1500 K (T_0 = 300 K).

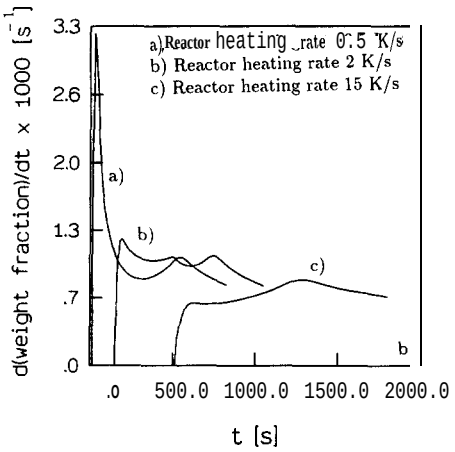

Fig. 6b. Time derivative of the weight fraction as function of time for several reactor heating rate [K s^{-1}] values and a final reactor temperature of 1500 K (T_0 = 300 K).

followed by a strong decrease, due to the process becoming heat transfer controlled. A new local maximum in the rate of weight loss is observed for the times of the particle heat-up. For very low heating rates (< 0.5 K s^{-1}), the rate of devolatilization shows a time dependence qualitatively similar to that simulated for high heating rates. However, the process on the whole is much smoother and the first peak is lower than the second one, simulated for conditions of final reactor temperatures (1500 K) and particle heat-up time. More complicated dynamics of particle weight loss are simulated for intermediate heating rates. Apart from a maximum in the rate of devolatilization, simulated at particle heat-up conditions, a region, delimited by two local maxima, is observed at the beginning of the process. The two maxima are due to the attainment of two characteristic temperature values at the surface of the particle,

that is the reaction temperature (550 K) and the final reactor temperature (1500 K), respectively.

The qualitative dependence of the instantaneous flux of gaseous products, at the particle surface, is similar to that of the rate of devolatilization, because of the negligible effects of the resistance to mass flow through the high-permeability char region. As expected, on the whole the devolatilization process is controlled by heat transfer. This is also confirmed by values of the ratio of the particle heat-up time to the time spent by the particle near the reaction temperature[10,18] close to unity.

The dependence of the product yields on the heating rate, expressed as a percentage of the initial weight of cellulose when 90% of the solid has been degraded, is shown in Fig. 7 for low (700 K), intermediate (1100 K) and high (1500 K) reactor temperatures. For low reactor temperatures, which do not allow secondary reactions to occur, product yields do not depend on the heating rate. A strong dependence is computed on the volatile distribution with little change in the char yield, for intermediate and high reactor temperatures. At very low heating rates, the heating time is longer than the total conversion time and the same product distribution is computed for T_r = 1100 K and T_r = 1500 K. As the heating rate increases, first the total gas yield is essentially the inverse of the tar yield, and then both volatile yields tend to constant values. The first trend is the result of enhanced secondary tar cracking due to the attainment of high temperature values within short times in the char region, effect which is stronger for very high final reactor temperatures. However, beyond certain temperatures, tar cracking cannot be further enhanced because of the reduced residence times and the almost total conversion to gas. Also, the small changes in the char yield, the product of primary reactions only, indicate that, even at high reactor temperatures, the changes in the heating rate do not cause significant variations in the selectivity of primary reactidns.

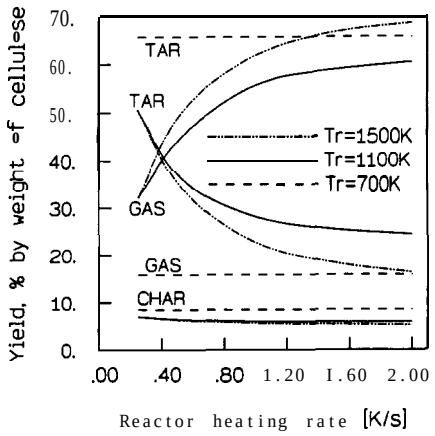

Fig. 7. Product yields, in percent by weight of cellulose when 99% of the solid has been degraded, and conversion time as functions of the reactor heating rate for T_r = 700, 1100 and 1500 K (T_0 = 300 K).

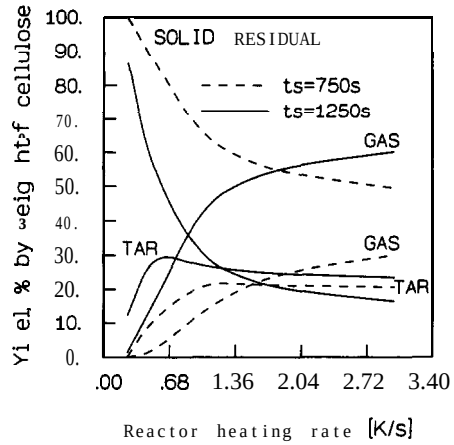

Fig. 8. Product yields, in percent by weight of cellulose when 90% of the solid has been degraded, as functions of the reactor heating rate for a reactor temperature of 1100 K and two particle residence times (T_0 = 300 K).

Further information on the effects of the heating rate on the conversion process can be obtained from Fig. 8, where the volatile yields and the solid residual are reported as functions of the heating rate for a final reactor temperature of 1100 K and for two particle residence times, that is, 750 s and 1240 s. It can be observed that the optimal tar yield (about 31%) is obtained for the longer particle residence time and for a heating rate of 0.5 K s^{-1}, with a solid residual of 50%. For slightly larger values of the heating rate, a slightly lower constant value of tar yield is predicted. This is the result of a balance between the effect of the increased reaction temperature and the reduced volatile residence times. Optimal gas yields are also obtained for the longer particle residence time for heating rates larger that 2 K s^{-1}, with a solid residual less than 20%. At short particle residence times, low yield of volatiles are obtained with tar prevailing at low heating rates and slight predominance of gas yields at intermediate and high heating rates.

The role of the reactor temperature on the conversion process and the extent of secondary reactions can be analyzed through Fig. 9, where the product yields, expressed as a percentage of

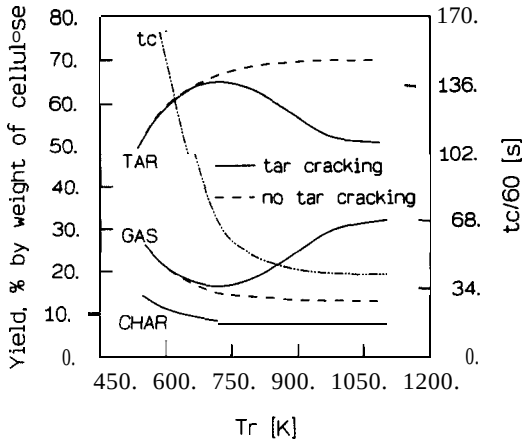

Fig. 9. Product yields,in percent by weight of cellulose when 90% of the solid has been degraded, and conversion time as functions of the reactor temperature for a reactor heating rate of 0.25 K s^{-1} with (solid lines) and without (dashed lines) secondary reactions (T_0 = 300 K).

the initial weight of cellulose when 90% of the solid has been degraded, and the time needed for cellulose conversion is reported as a function of the reactor temperature for a heating rate of 0.25 K s^{-1}, as simulated with (solid lines) and without (dashed lines) secondary reactions. For reactor temperatures below 750 K, secondary reactions do not occur and product distribution is the result of the selectivity between tar formation, on the one hand, and gas and char formation, on the other. Tar yield is always larger than char and gas yields even for very low temperatures (about 50% against 40% for T_r = 550 K). In the absence of secondary reactions, the tar yield increases with the reactor temperature while the char and gas yields decrease (dashed lines of Fig. 9) with the attainment of constant values for temperatures larger than 1000 K (about 7%, 12.5% and 70.5%, for char, gas and tar, respectively).

The solid lines of Fig. 9, obtained with secondary reaction effects, show an increase in the gas yield at the expense of tar and a slight decrease in the char yield for reactor temperatures larger than 750 K. For temperatures larger than 1100 K, product yields tend to constant values (about 10%, 30% and 50% for char, gas and tar, respectively), indicating that chemical reactions had taken place before the final reactor temperature had been reached. The negligible changes in the conversion times, computed with and without secondary reactions, suggest that the energetics of secondary reactions, as described by the present model, do not affect the conversion process significantly.

The coupled effects of the reactor temperature and heating rate on the product yields and conversion time can be observed from Fig. 10. It is confirmed that, at low reactor temperatures, the heating rates do not affect the product yields, which result only from primary reactions. The heating rate effects are, however, very important for high reactor temperatures (>900 K). In fact, for the highest heating rate, a strong increase in the gas yield at the expense of tar is observed from T_r = 900 K to T_r = 1300 K. For higher reactor temperatures, the tar cracking reaction is limited by the reduced residence times and concentration of tar available for the reaction to occur. A maximum of gas yield of about 77% and a minimum of tar yield of about 8% are predicted for T_r = 1500 K. The char yield slightly decreases with the reactor temperature, showing, for the highest heating rate, a decrease from 8.5% (T_r = 700 K) to 5% (T_r = 1500 K). The comparison of the curves of the char yield, product of primary reactions only, confirms that primary reaction pathways are scarcely affected by the heating rate. As expected, the conversion time decreases, for a fixed reactor temperature, as the heating rate is increased.

The effects of the reactor temperature on the devolatilization process, for a reactor heating rate of 15 K s^{-1}, can be observed from Figs 1 la and 11 b, through the solid weight fraction and its rate as functions of time. A significant amount of time lapses before the temperature inside the cellulose particle reaches sufficiently high values to cause the onset of the major degradation reactions. The particle heat-up time

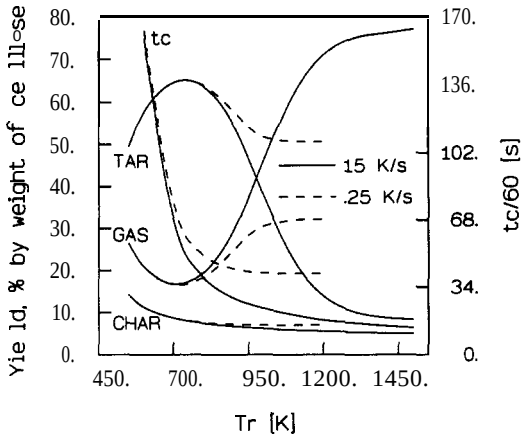

Fig. IO. Product yields, in percent by weight of cellulose when 99% of the solid has been degraded, and conversion time as functions of the reactor temperature for a heating rate of 15 K s^{-1} (solid lines) and 0.25 K s^{-1} (dashed lines) (T_0 = 300 K).

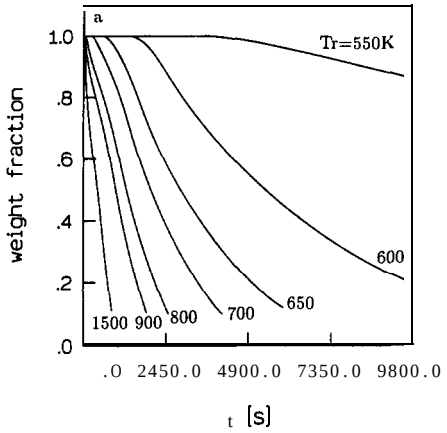

Fig. 1 la. Weight fraction as function of time for several reactor temperatures and for a reactor heating rate of 15 K s^{-1} ($T_0 = 300$ K).

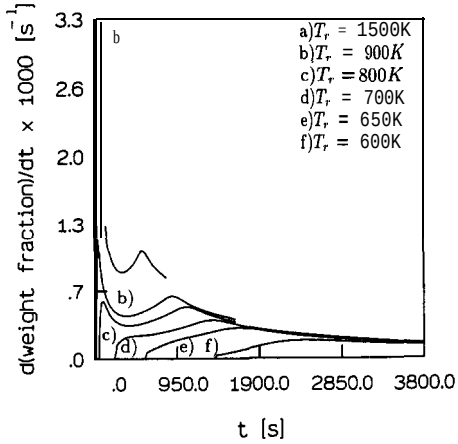

Fig. I[b. Time derivative of the weight fraction as function of time for several reactor temperatures and for a reactor heating rate of 15 K s^{-1}(T_0 = 300 K).

is shortened by increasing the reactor temperature. From the dynamics of the rate of weight loss it appears that, for the higher reactor temperatures (> 800 K), a first peak, due to the devolatilization of a narrow region close to the exposed fuel surface, is followed by a second local maximum at the time of the particle heat-up. As the reactor temperature is lowered, the first peak becomes barely visible, and the maximum rate of devolatilization is computed for long times, that is, again for times of very large reaction zones (heat-up times).

CONCLUSIONS

A model of cellulose pyrolysis, which couples the description of all main physical processes to a well-known mechanism of primary degradation of cellulose and secondary degradation of evolved pyrolysis products, has been presented. The model has been used to simulate the dependence of the conversion process on the reactor temperature and heating rate, as a first step towards the development of comprehensive biomass models based on the contributions of the single biomass components.

On the whole, the pyrolysis of large cellulose particles is always controlled by the heat transfer rate. Indeed, the analysis of a single particle pyrolysis for high reactor temperatures and heating rates has shown that, for very short times, the process is initially controlled by the rate of devolatilization. Then, the heat transfer from the reacting zone to the virgin cellulose region decreases with a decrease in the rate of volatile production. Primary pyrolysis of almost 1×10^{-2} m of the particle thickness was completed at temperatures below 650 K for all heating rates and final temperatures of the reactor that were investigated. Under these conditions, all primary reactions come to completion and the particle temperature in the already charred region does not affect the primary reaction pathways.

Vapor phase reactions are strongly affected by both the heating rate and the reactor temperature. Secondary tar cracking rate attains the maximum value when sufficiently high temperatures are established in the char region and high tar concentrations are available. As the heating rate is increased, high temperatures are reached in shorter times in the char region favoring the tar cracking. However, the rate of volatile species formation increases with larger gas overpressures and flow velocities. The reduced conversion times and the increased velocity values reduce the tar residence times so lowering the extent of the tar cracking reaction.

The simulations have been done for a chosen set of kinetic data and values of the heat of pyrolysis. An extensive study[14] of the effects of these parameters on wood pyrolysis has shown very high sensitivities in the tar yields for variations in the rates of its formation and cracking. A similar behavior can also be expected for cellulose pyrolysis, indicating possible changes in the conclusions, mainly in the role played by secondary reactions.

The effects of the reactor heating rate and reactor temperature on cellulose pyrolysis have been experimentally investigated (see for instance Refs [16, 18, 19, 25–29]), mainly to determine the kinetic data. In few cases, product distributions from small (about 0.01 x 10^{-2} m) cellulose particle pyrolysis, for reactor tempera-

tures of 700-1100 K[18] and 600-1400 K[27] have also been made available. These are, of course, strongly affected by the different residence times, therefore a direct comparison among the two sets of experimental data and those simulated by this numerical model cannot be made. However, in general, it can be observed that secondary reactions are always important for the conditions of Ref. [18] where the optimal tar yield is obtained at the lowest reactor temperature (700 K). This finding is in close agreement with the predictions of the numerical model. Again, in agreement with Ref. [18] the predicted gas yield, at high heating rates and for a wide range of the reactor temperatures (800-l 100 K), is essentially the inverse of the tar yield, with negligible char formation except at very low reactor temperatures.

In Ref. [27] the cellulose degradation was seen to begin between 570 and 670 K and most of the weight loss to take place between 770 and 970 K. Tar yield increases with the peak temperature to a maximum for T_r = 970 K. For higher temperatures, secondary reactions become important. The numerical model, according to Ref. [27], has shown that, for low reactor temperatures (T_r < 700 K), the gas yield is always lower than the tar yield, but the decrease of the gas yield, in the region of increasing tar yield, the result of the selectivity of primary reactions, is not observed experimentally because of the much shorter solid residence times. Furthermore, for large cellulose particles, even under extreme conditions of temperature and heating rates, even though the rate of the reaction (a3) (tar formation) predominates over that of reaction (a2) (gas and char formation), total conversion of the particle to volatiles, as shown by experiments conducted at very high heating rate, for small strips of cellulose,[26] never occurs in the model.

Acknowledgements-The work was supported by the European Economic Community under Contract Joule No. 0035 and by the National Research Council of Italy under Contribution N.91/2386 and N.91/2236.

NOMENCLATURE

A_i	Pre-exponential factor
c	Heat capacity
D	Diffusion coefficient
d	Pore diameter
E_i	Activation energy
e	Surface emissivity
h	Specific enthalpy per unit mass
h_{conv}	Convective heat transfer coefficient
K	Permeability
k	Thermal conductivity
L	Particle half thickness
M	Mass
P	Gas overpressure (over p_0)
p	Gas pressure
q	Intensity of the radiative heat flux
R	Universal gas constant
T	Temperature
T_r	Final reactor temperature
T_{rea}	Reactor temperature
$T0$	Reference temperature
t	Time
t_c	Conversion time
u	Gas velocity
V	Volume
W_g	Mean molecular weight
x	Space
Y_T	Tar mass fraction

Greek letters

ρ	Mass concentration
ϵ	Porosity
Δh	Heat of reaction
μ	Viscosity
ν	Stoichiometric coefficient
η	$(M_W + M_A)/M_{W0}$
σ	Stefan-Boltzmann constant
ω	Emissivity

Subscripts

A	Active cellulose
C	Char
G	Gas
g	total volatile species (gas + tar)
i	ith chemical species
k	k th chemical reaction
T	Tar
W	Cellulose
0	ambient value

REFERENCES

1. C. A. Koufopanos, G. Maschio and A. Lucchesi, Kinetic modelling of the pyrolysis of biomass and biomass components. ***Can. J. Chem. Engng 67, 75-84 (1989).***
2. ***S. S.*** Alves and J. L. Figueiredo, Pyrolysis kinetics of lignocellulosic materials by multistage isothermal thermogravimetry. ***J. Anal. Appl. Pyrolysis 13, 123 (1988).***
3. S. W. Ward and J. Braslaw, Experimental weight loss kinetics of wood pyrolysis under vacuum. ***Combustion and Flame 61, 261-269 (1985).***
4. ***C.*** Vovelle H. Mellotte and R. Delburgo, Kinetics of the thermal degradation of cellulose and wood in inert and oxidative atmospheres. ***Nineteenth Symp. (Int.) on Combustion, The Combustion Institute,*** pp. 797-805 (1982).
5. P. T. Williams and S. Besler, Thermogravimetric analysis of the components of biomass. ***Proc. Int. Conf. Advances in Thermochemical Biomass Conversion,*** Interlaken (A. S. Bridgwater ed.), pp. 771-783 (1994).
6. J. Lédé. J. Panagopoulos. H. Z. Li and J. Villermaux. Fast pyrolysis of wood: direct measurements and study of ablation rate. ***Fuel 64,*** 1514–1520 (1985).
7. H. A. Kung, A mathematical model of wood pyrolysis. ***Combustion and Flame 18, 185-195 (1972).***
8. E. J. Kansa, H. E. Perlee and R. F. Chaiken, Mathematical model of wood pyrolysis including internal forced convection. ***Combustion and Flame 29, 31 l-324 (1977).***
9. J. Villermaux, B. Antoine, J. Lédé and F. Soulignac, A new model for thermal volatilization of solid particles undergoing fast pyrolysis. ***Chem. Engng Sci.*** **41,** 15 l-l 57 (1986).

10. V. Kothari and M. J. Antal, Numerical studies of the flash pyrolysis of cellulose. *Fuel 64,* 1487-1494 (1985).
11. I. S. Wichman and M. Melaan, Modeling the pyrolysis of cellulose and wood. *Proc. Int. Conf. Advances in Thermochemical Biomass Conversion,* Interlaken (A. S. Bridgwater ed.), pp. 887-905 (1994).
12. L. J. Curtiss and D. J. Miller, Transport model with radiative heat transfer for rapid cellulose pyrolysis. *Ind. Engng Chem. Res. 27, 1775-1783 (1988).*
13. W. R. Chan, M. Kelbon and B. B. Krieger, Modelling and experimental verification of physical and chemical processes during pyrolysis of large biomass particle. *Fuel 64,* 15051513 (1985).
14. C. Di Blasi, Analysis of convection and secondary reaction effects within porous solid fuels undergoing pyrolysis. *Combustion Sci. Technol. 90, 3 15-339 (1993).*
15. F. Thurner and U. Mann, Kinetic investigation of wood pyrolysis. *Ind. Engng Chem. Process Des. Dev.* 20, 482428 (1981).
16. A. G. W. Bradbury, Y. Sakai and F. Shafizadeh, A kinetic model for pyrolysis of cellulose. *J. Appl. Polym. Sci.* 23, 3271-3280 (1979).
17. A. G. Liden, F. Berruti and D. S. Scott, A kinetic model for the production of liquids from the flash pyrolysis of biomass. *Chem.* Engng *Comm.* 65, 207-221 (1988).
18. D. S. Scott, J. Piskorz, M. A. Bergougnou, R. Graham and R. P. Overend, The role of temperature in the fast pyrolysis of cellulose and wood. *Ind. Engn. Chem. Res.* 27, 8–15 (1988).
19. F. J. Kilzer and A. Broido, Speculation on the nature of cellulose pyrolysis *Pyrodynamics 2,* 15 1-163 (1965).
20. D. F. Arseneau, Competitive reactions in the thermal decomposition of cellulose. Can. *J. Chem.* 49, 632-638 (1971).
21. M. J. Antal, Effects of reactor severity on the gas-phase pyrolysis of cellulose- and kraft lignin-derived volatile matter. *Ind. Engng Prod. Res. Dev. 22, 366375 (1983).*
22. M. L. Boroson, J. B. Howard, J. P. Longwell and A. W. Peters, Products yields and kinetics from the vapor phase cracking of wood pyrolysis tars. *AIChE J. 35,* 120–128 *(1989).*
23. C. K. Lee, R. F. Chaiken and J. M. Singer, Charring pyrolysis of wood in fires by laser simulation. *Sixteenth Symp. (Int.) on Combustion,* The Combustion Institute, Pittsburgh, PA, pp. 1459-1470 (1976).
24. R. Bilbao, A. Millera and M. B. Murillo, Heat transfer and weight loss in the thermal decomposition of large wood particles. *Proc. Int. Conf. Advances in Thermochemical Biomass Conversion* (A. S. Bridgwater ed.), pp. 874886 (1994).
25. M. J. Antal, H. L. Friedman and F. E. Rogers, Kinetics of cellulose pyrolysis in nitrogen and steam. *Combustion Sci. Technoi.* 21, 141-152 (1980).
26. P. C. Lewellen, W. A. Peters and J. B. Howard, Cellulose pyrolysis kinetics and char formation mechanism. *Sixteenth Symp. (Int.) on Combustion,* The Combustion Institute; Pittsburgh, PA, pp. 1471-1480 (1976).
27. M. R. Haialigol, J. B. Howard. J. P. Lonawell and W. A. Peters:Product compositions and kinetics for rapid pyrolysis of cellulose. *Ind. Engng Chem. Process Des. Dev.* 21, 457465 (1982).
28. A. Tabatabaie-Raissi, W. S. L. Mok and M. J. Antal, Cellulose pyrolysis kinetics in a simulated solar environment. *Ind. Engng Chem. Res.* **28,** 856865 (1989).
29. B. K. Gullet and P. Smith. Thermogravimetric study of the decomposition of pelletized cellulose at 315°C–800°C. *Combustion and Flame 67, 143-151 (1987).*